

## **Supplementary Material**

# **Lasing Action in Microdroplets Modulated by Interfacial Molecular Forces**

Zhen Qiao,<sup>a</sup> Xuerui Gong,<sup>a</sup> Peng Guan,<sup>b</sup> Zhiyi Yuan,<sup>a</sup> Shilun Feng,<sup>c</sup> Yiyu Zhang,<sup>a</sup>

Munho Kim,<sup>a</sup> Guo-En Chang,<sup>d</sup> Yu-Cheng Chen<sup>a,e,\*</sup>

<sup>a</sup> School of Electrical and Electronic Engineering, Nanyang Technological University, 50  
Nanyang Avenue, 639798, Singapore

<sup>b</sup> School of Electronic Information and Electrical Engineering, Shanghai Jiao Tong  
University, Shanghai 200240, China

<sup>c</sup> State Key Laboratory of Transducer Technology, Shanghai Institute of Microsystem  
and Information Technology, Chinese Academy of Sciences, Shanghai, 200050, China

<sup>d</sup> Department of Mechanical Engineering, National Chung Cheng University, Minhsiung,  
Chiayi 62102, Taiwan, ROC

<sup>e</sup> School of Chemical and Biomedical Engineering, Nanyang Technological University,  
62 Nanyang Drive, 637459, Singapore

## Section 1

### Lasing threshold calculation under different dye concentrations.

The lasing threshold of a FITC-doped droplet laser is calculated based on rate equations which describe the dynamics of intra-cavity photons and populations of dye<sup>40</sup>:

$$\begin{aligned}\frac{dn(t)}{dt} &= I_p(t)\sigma_{ap}[N_0 - n(t)] - \frac{\sigma_{el}c}{\eta}n(t)q(t) + \frac{\sigma_{al}c}{\eta}[N_0 - n(t)]q(t) - \frac{n(t)}{\tau_f} \\ \frac{dq(t)}{dt} &= \frac{Fc}{\eta V}\sigma_{el}n(t) + \frac{F\sigma_{el}c}{\eta}n(t)q(t) - \frac{F\sigma_{al}c}{\eta}[N_0 - n(t)]q(t) - \frac{q(t)}{\tau_q}\end{aligned}\quad (S1)$$

In Eq. S1,  $n$  is the spatially averaged density of FITC molecules in the first excited state;  $q$  is the photon density at the lasing wavelength;  $I_p$  is the pump intensity;  $N_0$  is the total concentration of FITC molecules;  $\sigma_{ap}$  is the absorption cross section at pump wavelength;  $\sigma_{el}$  is the emission cross section at lasing wavelength;  $\sigma_{al}$  is the absorption cross section at lasing wavelength;  $\tau_f$  is the fluorescent lifetime of FITC;  $\eta$  is the refractive index of a droplet resonator;  $F$  is the fraction of mode volume occupied by the dye molecules;  $V$  is the volume of the electromagnetic mode;  $h$  is Planck's constant;  $c$  is the light velocity; and  $\tau_q$  is the photon lifetime of cavity. Note that  $\tau_q = Q\lambda_l/(2\pi c)$ , where  $Q$  is the Q-factor of a droplet resonator; and  $\lambda_l$  is the lasing wavelength. Details of the parameters in Eq. S1 are summarized in Table. S1. Considering a Gaussian temporal profile of pump intensity  $I_p = I_{p0} \cdot \exp[-4 \cdot \ln 2 \cdot (t/\Delta t)^2]$ , the pump energy density<sup>41</sup> is  $\Phi_p = hc\Delta t I_{p0}/(0.94\eta_p\lambda_p)$ .  $\Delta t$  is the pump pulse width,  $\lambda_p$  is the pump wavelength and  $\eta_p$  is the pump efficiency.

By numerically solving Eq. S1, we can calculate the time-integrated photon density at the lasing wavelength as a function of pump energy density. As a consequence, the corresponding lasing threshold can be obtained. Based on such calculation process, we obtained the lasing thresholds under different FITC concentrations. As shown in Fig. S5b, the calculated lasing thresholds (red line) have a good agreement with the experiment data. The results indicate that the thresholds of lasing actions are consistent with the magnitudes of the gain and with the resonator losses.

## Section 2

### Calculation of droplet-solid interfacial tension and capillary length

The droplet-solid interfacial tensions in Fig. 4 are calculated according to the well-known Young equation<sup>34</sup> and the equation of state (EoS) developed by Neumann *et al*<sup>35</sup>. According to Young equation, the following relationship is satisfied:

$$\gamma_l \cos \alpha = \gamma_s - \gamma_i \quad (\text{S2})$$

Where  $\gamma_l$  is the droplet surface tension,  $\alpha$  is the droplet contact angle,  $\gamma_s$  is the solid surface tension, and  $\gamma_i$  is the interfacial tension. According to EoS,  $\gamma_l$ ,  $\gamma_s$ , and  $\gamma_i$  satisfy the following relationship:

$$\gamma_i = \gamma_s + \gamma_l - 2\sqrt{\gamma_s \gamma_l} e^{-\beta(\gamma_l - \gamma_s)^2} \quad (\text{S3})$$

Where  $\beta$  is an empirical constant that was found to be 0.0001247. Considering that the water/glycerol ratio of the droplets in Fig. 4 is 1:1, the droplet surface tension  $\gamma_l$  is calculated to be 68.04 [mN/m]<sup>36</sup>. Then the interfacial tension  $\gamma_i$  at a specific contact angle can be obtained (Fig. 4) by numerically calculating Eq. S2 and S3.

As for the interfacial tensions in Fig. 5b, the solid surface tension  $\gamma_s$  is first obtained to be 26.97 mN/m according to Eq. S2 and S3 under the BSA concentration of 0. Note that for the BSA concentration of 0, the droplet surface tension is estimated to be 67.35 mN/m given the PBS/glycerol ratio of 3:1<sup>36,38</sup>. In the process of biomolecular adsorption, there are no biomolecules outside a droplet, thus the solid surface tension remains constant which is independent of the biomolecular concentration. Then, the interfacial tension  $\gamma_{i,BSA}$  under different BSA concentrations can be obtained according to Eq. S2:

$$\gamma_{i,BSA} = \gamma_s - \gamma_{l,BSA} \cos \alpha_{BSA} \quad (\text{S4})$$

Where  $\alpha_{BSA}$  is the droplet contact angle within BSA (Fig. 5b);  $\gamma_{l,BSA}$  is the surface tension of droplet within BSA.  $\gamma_{l,BSA}$  is estimated to be 67.35 mN/m (concentration of BSA  $\leq 15$  nM) and 56.03 mN/m (concentration of BSA  $\geq 150$  nM)<sup>36,38,39</sup>.

The capillary length of a droplet is given by the following formular<sup>43</sup>:

$$l_c = \sqrt{\gamma / \rho g} \quad (\text{S5})$$

where  $l_c$  is the capillary length;  $\gamma$  is the surface tension of a droplet;  $\rho$  is mass density of a droplet and  $g$  is the gravitational acceleration. Here we estimate the capillary length of a droplet with a water/glycerol volume ratio of 1:1. The surface tension of such a droplet is 68.04 mN/m. The mass density is estimated to be 1.14 [g/cm<sup>3</sup>]<sup>44</sup>. The gravitational acceleration is 9.8 m/s<sup>2</sup>. According to Eq. S5, the capillary length of a droplet with a water/glycerol volume ratio of 1:1 is estimated to be 2.5 mm. The sizes of the droplets in this work are micron scale, which are far smaller than the capillary length. Therefore, the shapes of the droplets are governed mostly by surface tension and the surfaces are nearly spherical.

### Section 3

#### Calculation of FSRs of AL modes and the maximum number of AL oscillation paths

For calculating the FSR of an AL mode and the maximum number of AL oscillation paths, the geometry of an AL oscillation path in a droplet is analyzed. As an example, Fig. S6 presents the side-view geometry of a droplet resonator and an AL oscillation path that follows N-sided polygon with N=8. The droplet (sky blue region in Fig. S6) possesses a diameter of  $D$  and a contact angle of  $\alpha$ . The N-sided polygon path possesses a side length of  $l$  (blue marked in Fig. S6). According to the law of reflection, the polygon sides at the two ends of the droplet are perpendicular to the droplet bottom, presenting two short sides with the length of  $h$  (green marked in Fig. S6). Thus, the optical path length of an AL mode with N in a round trip is:

$$L = 2n \times \left[ \left( \frac{N}{2} - 1 \right) l + 2h \right] \quad (\text{S6})$$

Where  $L$  is the optical path length,  $n$  is the effective refractive index of the droplet, and N is the side number of an N-sided polygon. Because the radius of the circle containing the droplet profile (black circle in Fig. S6) is  $R = D / (2 \sin \alpha)$ , the side length  $l$  of the N-sided polygon is [see Fig. S6]:

$$\begin{aligned} l &= R \sin(\pi / N) \times 2 \\ &= \frac{\sin(\pi / N)}{\sin \alpha} D \end{aligned} \quad (\text{S7})$$

As depicts in Fig. S6, the length of the two short sides  $h$  can be calculated as:

$$\begin{aligned}
 h &= l/2 - d \\
 &= \frac{\sin(\pi/N)}{2 \sin \alpha} D - R \cos \alpha \\
 &= \frac{\sin(\pi/N)}{2 \sin \alpha} D - \frac{D}{2 \tan \alpha}
 \end{aligned} \tag{S8}$$

Substituting Eq. S7 and Eq. S8 into Eq. S6, the optical path length of an AL mode with  $N$  in a round trip can be calculated as:

$$L = \left[ \frac{N \sin(\pi/N) - 2 \cos \alpha}{\sin \alpha} \right] nD \tag{S9}$$

Then, the FSR of an AL mode with  $N$  can be obtained:

$$FSR = \frac{c}{L} = \frac{c \sin \alpha}{\left[ N \sin(\pi/N) - 2 \cos \alpha \right] nD} \tag{S10}$$

Where  $c$  is the speed of light. When an AL mode with  $N$  is permitted to oscillate in a droplet, the following relationship between  $\beta$  [purple marked in Fig.S6] and the contact angle  $\alpha$  must be satisfied:

$$\beta = \angle AOB = \frac{N-2}{2N} \pi < \alpha \tag{S11}$$

According to Eq. S11, the maximum permitted  $N$  under a specific contact angle can be obtained:

$$N_{\max} = 2 \times \left[ \frac{\pi}{\pi - 2\alpha} \right] \tag{S12}$$

Considering that  $N$  is an even, the maximum number of AL oscillation paths under a specific contact angle can be calculated as:

$$n_{AL} = \frac{N_{\max}}{2} - 1 = \left[ \frac{\pi}{\pi - 2\alpha} \right] - 1 \tag{S13}$$

The theoretical curve calculated according to Eq. S13 is shown in Fig. 4(d) of the manuscript.

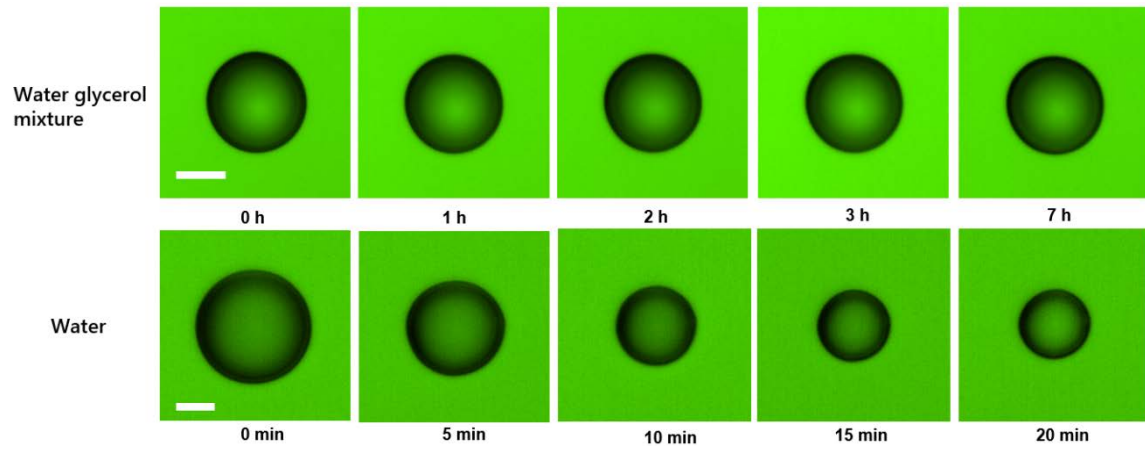


**Fig. S1.** Top-view profiles of a water/glycerol droplet (top) and a water droplet (below) over time. The volume ratio of the water/glycerol is 1:1.

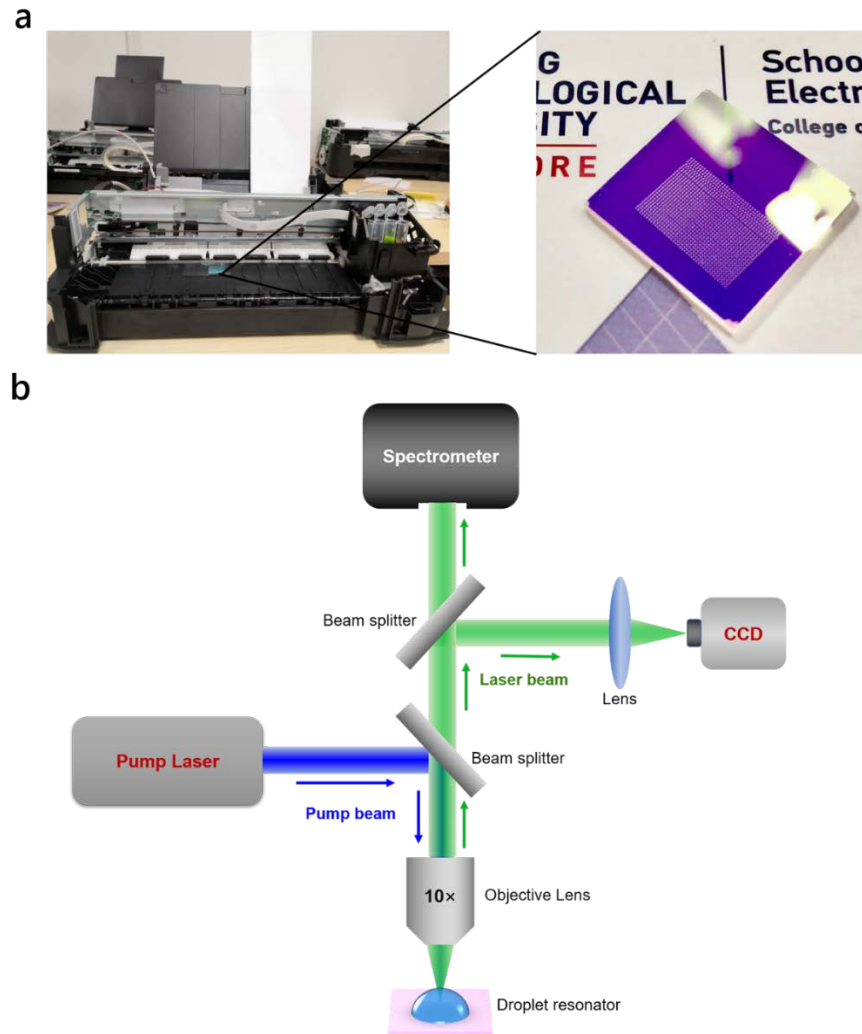


**Fig. S2.** (a) Image of the office inkjet printer (left). Image of the mirror printed droplets on the surface (right). (b) Schematic of the optical system for droplet lasers.

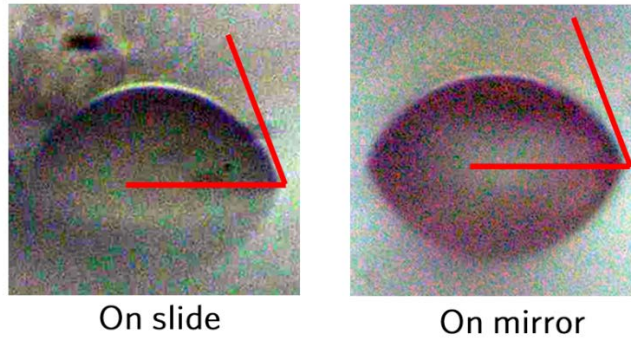


**Fig. S3.** Side-view profiles of a droplet on the slide (**left**) and a droplet on the mirror (**right**). The contact angles of the droplets are both  $69^\circ$ , indicating the identical hydrophobicity of the slide and the mirror.

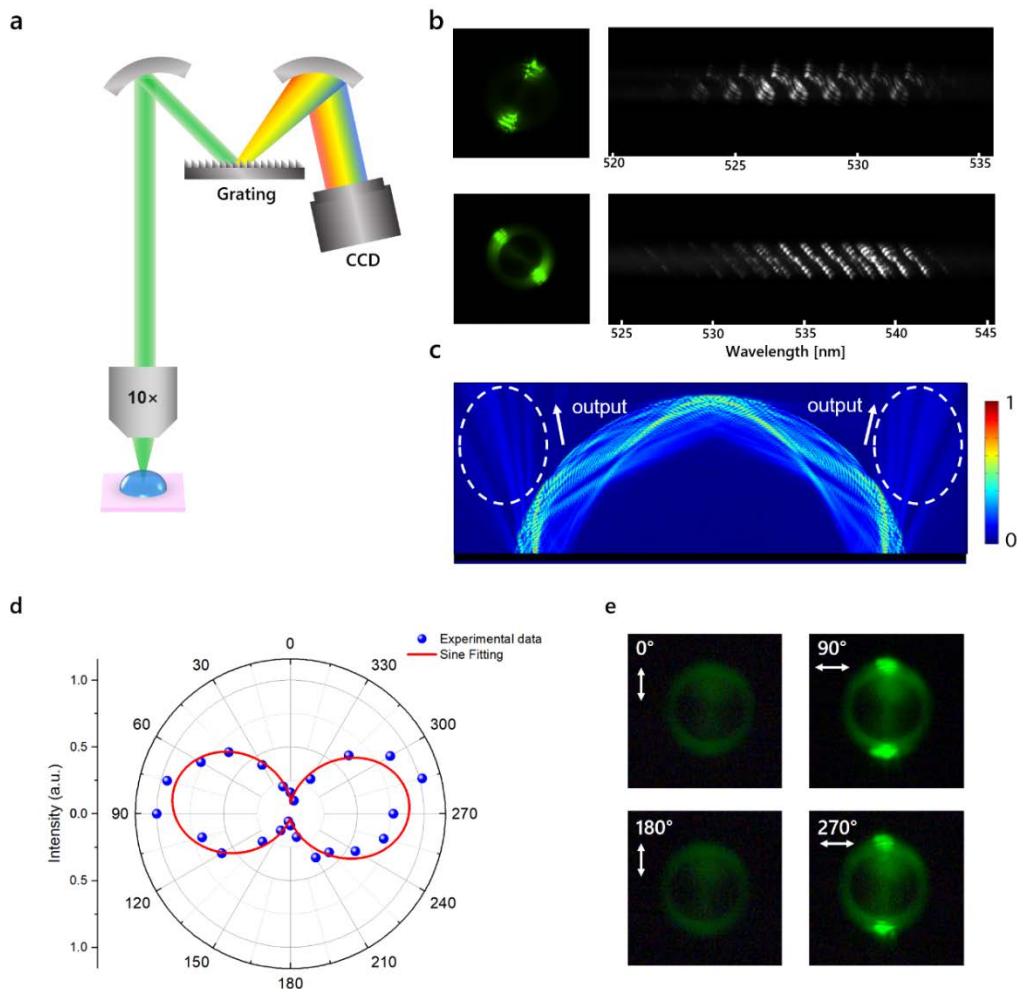


**Fig. S4.** (a) Schematic of an imaging spectrometer. A laser beam generated from a droplet is collimated by an objective lens, then incident on a grating. After diffracted by the grating, the laser modes with different wavelengths from the same laser beam are imaged by a CCD. (b) Optical images of droplet lasers (left) and the laser modes with different wavelengths diffracted by the grating (right). (c) Simulation of a laser beam output from two ends of a droplet. (d) Intensities of droplet lasers filtered by a polarizer under different polarization directions. The experimental dots are well fitted by sine function, indicating that the output laser beam is a linearly polarized light. (e) Optical images of droplet lasers filtered by the polarizer with polarization directions of  $0^\circ$ ,  $90^\circ$ ,  $180^\circ$  and  $270^\circ$ . The polarization direction shown in (e) demonstrates TE mode lasing in the droplet, in which the laser polarization direction is parallel to the droplet surface. Simulation parameters: contact angle:  $79^\circ$ ; droplet diameter:  $55\ \mu\text{m}$ ; refractive index (RI) of the droplet: 1.41.

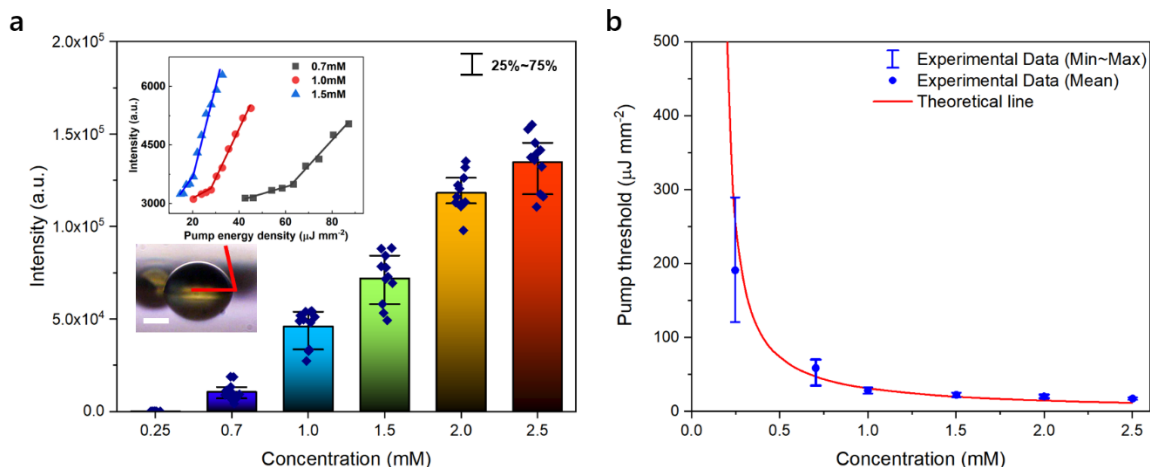


**Fig. S5.** (a) Statistics of spectrally integrated laser outputs at different FITC concentrations. Insets: spectrally integrated laser outputs as a function of pump energy density at FITC concentrations of 0.7 mM, 1.0 mM, and 1.5 mM (Top); side-view profile of a droplet with a contact angle of  $79^\circ$  (Below). Scale bar in the inset:  $20\ \mu\text{m}$ . Pump energy density:  $130\ \mu\text{J}/\text{mm}^2$ . (b) Lasing thresholds as a function of FITC concentration. Blue dots: experimental data. Red line: theoretical line calculated based on rate equations (Eq. S1).

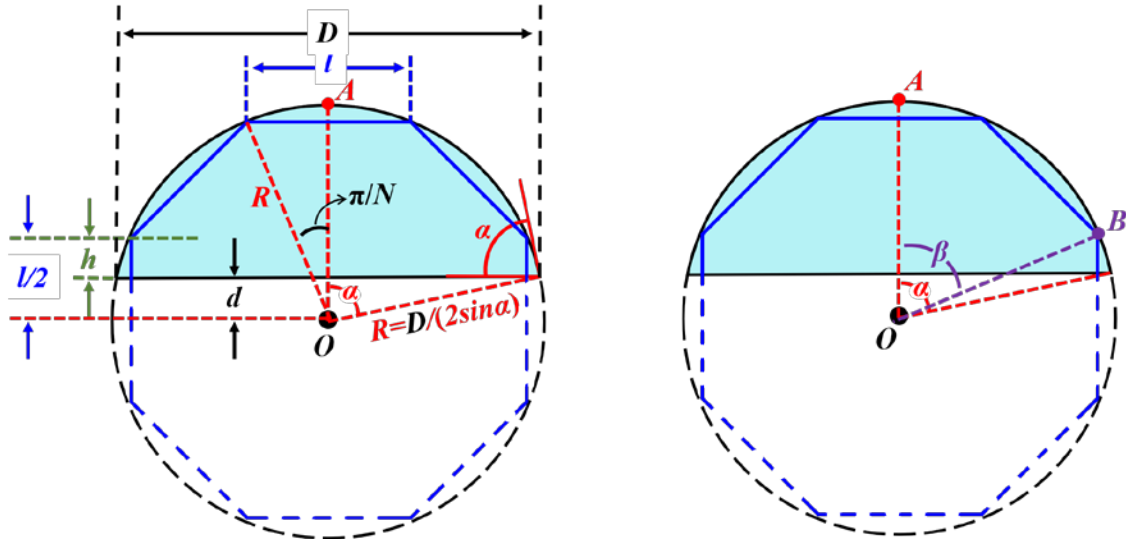


**Fig. S6.** Side-view geometry structure of a droplet and an AL oscillation path with  $N=8$  as an example. Sky blue region, side-view profile of a droplet resonator. Black dashed circle, supplemented circle of the droplet profile.  $D$ , diameter of a droplet.  $\alpha$ , contact angle. Black center dot “O”, circle center. Red dot “A”, point of intersection between center vertical line and the droplet profile. Blue solid line, oscillation path of an AL mode with  $N=8$  in a droplet. Blue dashed line, supplemented  $N$ -sided polygon of the oscillation path.  $l$ , side length of an  $N$ -sided polygon. Purple point “B”, the closest reflection point to the droplet bottom.  $\beta = \angle AOB$ . The left and right images represent the same droplet.

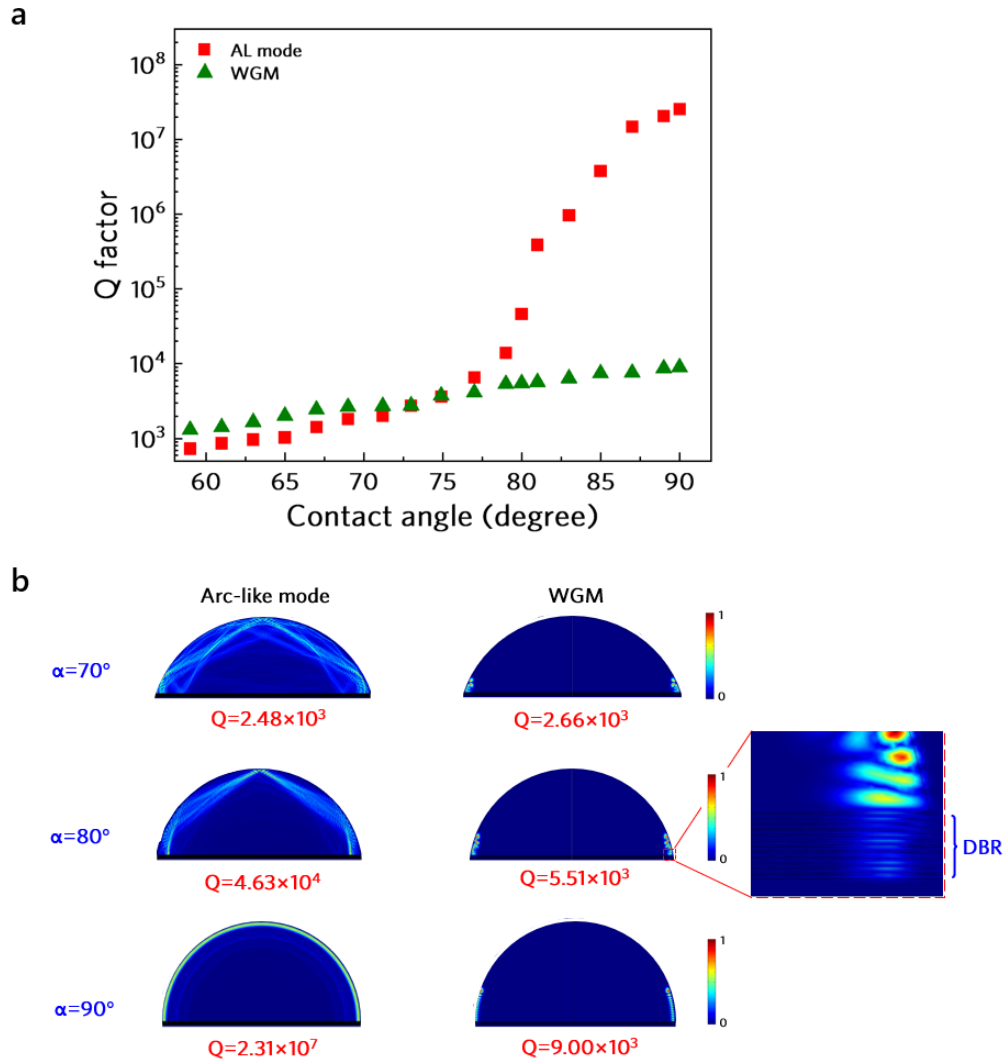


**Fig. S7. (a)** Calculated Q-factors of arc-like modes and WGM as a function of contact angle. The Q-factors under each contact angle in the figure are the maximum values selected from 100 solutions around 540 nm wavelength obtained by Comsol Multiphysics Software. **(b)** Simulated normalized electric field distribution of arc-like modes and WGM inside droplets with contact angles of  $70^\circ$ ,  $80^\circ$  and  $90^\circ$ , respectively. DBR: distributed Bragg reflector. As depicts in the zoomed region, a part of energy will be coupled into the DBR layers, resulting in a lower Q-factor of a WGM. Volume of the droplets: 68.5 pL. RI of droplets: 1.41. The DBR is composed of 24 dielectric layers alternating between high-RI (2.32) and low-RI (1.38) layers. The thickness of the high-RI layers is 58.2 nm; and the thickness of the low-RI layers is 97.8 nm.

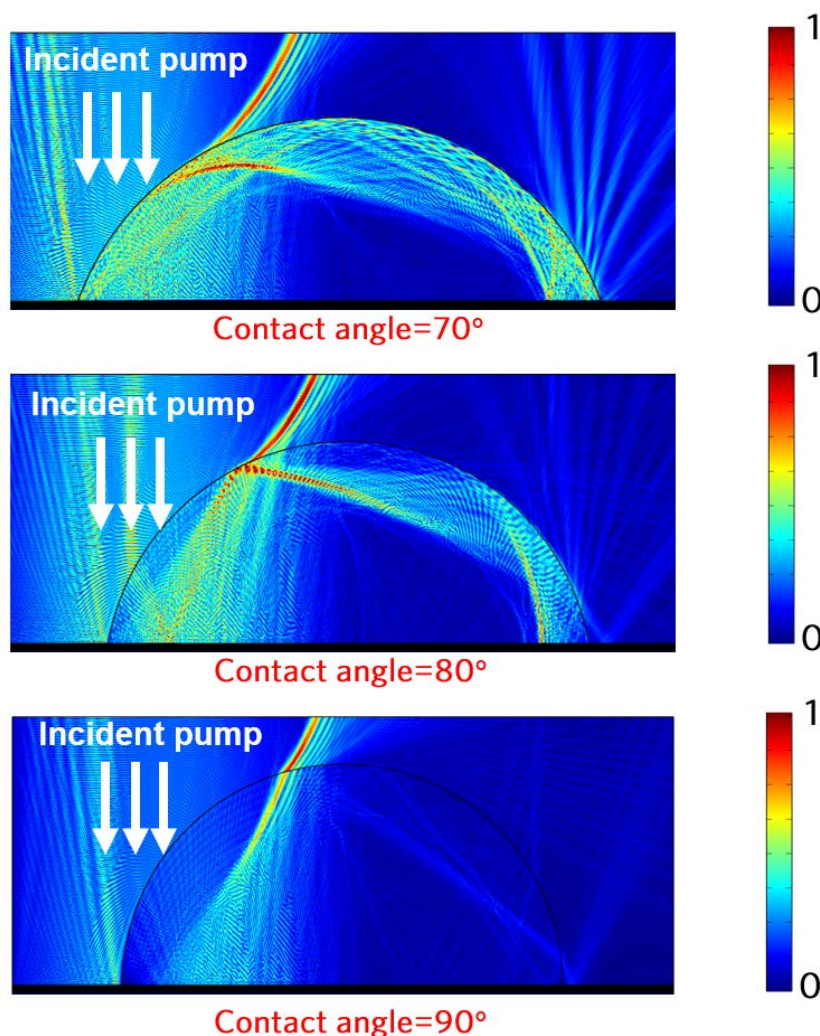


**Fig. S8.** Simulated pump light field distributions in droplets with contact angle of  $70^\circ$ ,  $80^\circ$ , and  $90^\circ$ . The pump light in droplets distributes along the droplet-air interface owing to the reflections between the mirror and droplet surface. The pump light field distributions were calculated using Comsol Multiphysics software, in which 2D model was employed. The Frequency Domain Study was applied in the Electromagnet Waves, Frequency Domain interface within the Wave Optics modules. The bottom DBR parameters are the same as those in Fig. S7. The pump beam was considered as a Gaussian beam with a beam waist radius of  $20\ \mu\text{m}$ . The beam waist is in the droplet bottom plane. Volume of the droplets:  $68.5\ \text{pL}$ . Pump wavelength:  $479\ \text{nm}$ . RI of droplets: 1.41.

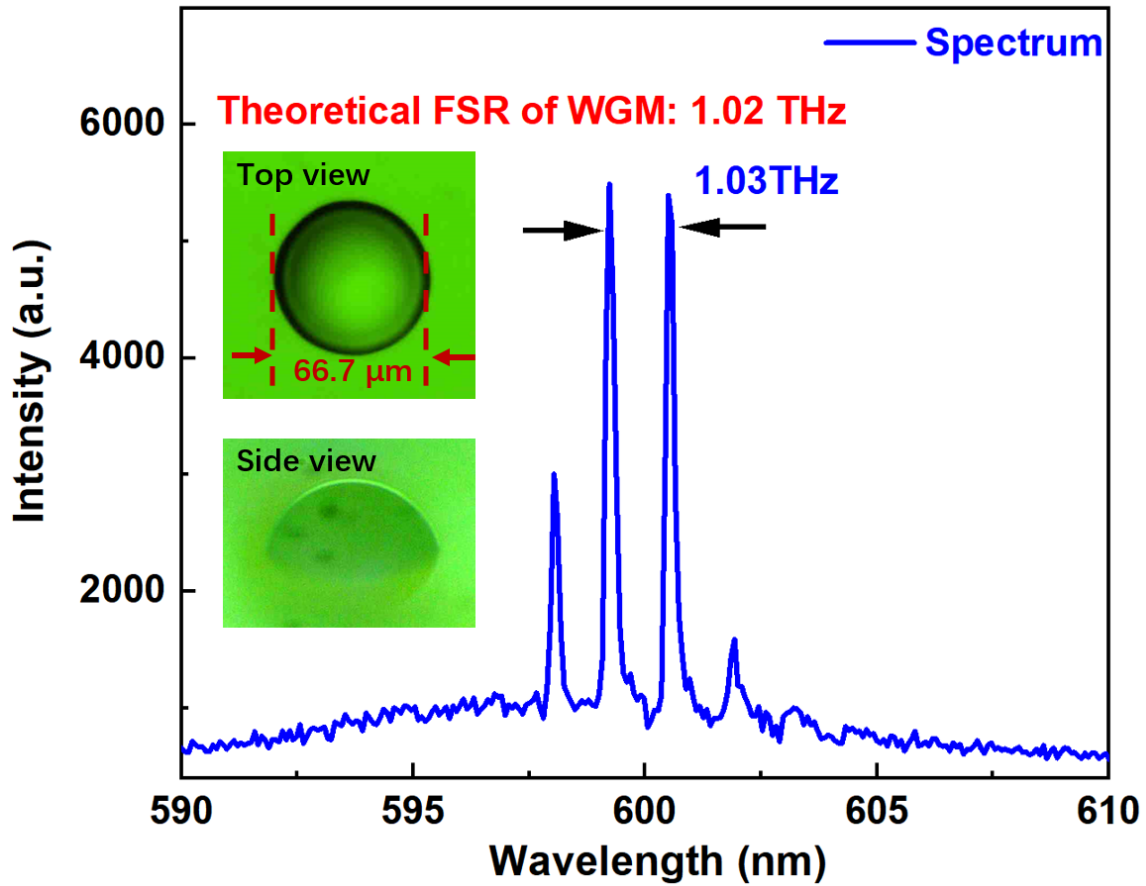


**Fig. S9.** Lasing spectrum of WGM from an RhB-doped droplet on a purple mirror. The reflectivity of the purple mirror at the emission wavelength of RhB dye is  $\sim 10\%$ . The FSR was measured to be 1.03 THz, which is close to the theoretical FSR of WGM:  $c/n\pi D=1.02$  THz.  $n$  ( $=1.41$ ) is the refractive index;  $D$  ( $=66.7 \mu\text{m}$ ) is the droplet diameter. Contact angle of the droplet:  $80^\circ$ .

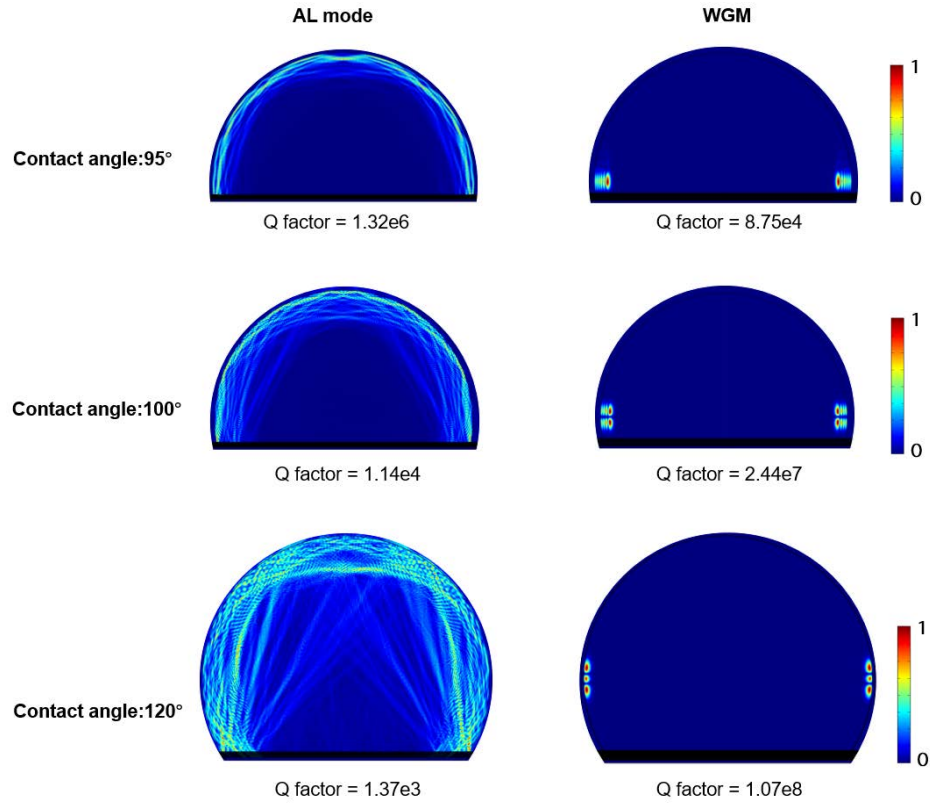


**Fig. S10.** Simulated normalized electric field distributions and calculated Q-factors of AL modes and WGM inside droplets with contact angles of 95°, 100° and 120°, respectively. Volume of the droplets: 68.5 pL. RI of droplets: 1.41

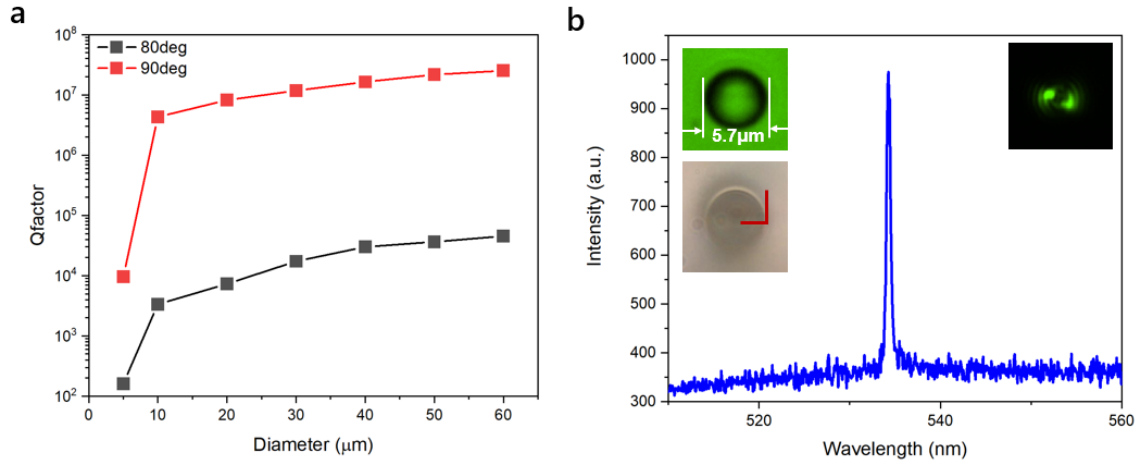


**Fig. S11. (a)** Q-factors of AL modes as a function of droplet diameter under contact angles of  $80^\circ$  and  $90^\circ$ . **(b)** lasing spectrum of a droplet with a  $5.7\text{-}\mu\text{m}$  diameter and a contact angle of  $90^\circ$ . Insets: top-view and side-view profiles of the droplet (left); optical image of the droplet laser (right).

**Table. S1**

Variables or Parameters	Description	value
$n$	Spatially averaged density of FITC molecules in the first excited state	
$q$	Photon densities at the lasing wavelength	
$I_p$	Pump intensity	
$N_0$	Total concentration of FITC molecules	
$\sigma_{ap}$	Absorption cross section at pump wavelength <sup>40</sup>	$1.25 \times 10^{-16} \text{ cm}^2$
$\sigma_{el}$	Emission cross section at lasing wavelength <sup>40</sup>	$1.19 \times 10^{-16} \text{ cm}^2$
$\sigma_{al}$	Absorption cross section at lasing wavelength <sup>40</sup>	$0.5 \times 10^{-19} \text{ cm}^2$
$\tau_f$	Fluorescent lifetime <sup>40</sup>	4.1 ns
$\Delta t$	Pump pulse width	5 ns
$c$	Light velocity	$3 \times 10^8 \text{ m/s}$
$h$	Planck's constant	$6.62606957 \times 10^{-34} \text{ J}\cdot\text{s}$
$\eta$	Refractive Index	1.41
$F$	Fraction of mode volume occupied by the dye molecules	1
$V$	Volume of the electromagnetic mode	$6.5 \times 10^{-10} \text{ cm}^3$
$\lambda_p$	Pump wavelength	479nm
$\lambda_l$	Lasing wavelength	540nm
$Q$	Q-factor	$1.4 \times 10^4$
$\tau_q$	Photon lifetime of cavity	$Q\lambda_l / (2\pi c)$
$\eta_p$	Pump efficiency	43%